Published in final edited form as:
Mol Biosyst. 2012 August ; 8(8): 2097–2105. doi:10.1039/c2mb25142f.

Coenzyme depletion by members of the aerolysin family of pore-forming toxins leads to diminished ATP levels and cell death†

Christine M. Fennessey[a,b], **Susan E. Ivie**[a,b], and **Mark S. McClain**[a]

Mark S. McClain: mark.mcclain@vanderbilt.edu

[a]Division of Infectious Disease, Department of Medicine, Vanderbilt University School of Medicine, Nashville, Tennessee, United States of America.

Abstract

Recent studies demonstrated that a variety of bacterial pore-forming toxins induce cell death through a process of programmed necrosis characterized by the rapid depletion of cellular ATP. However, events leading to the necrosis and depletion of ATP are not thoroughly understood. We demonstrate that ATP-depletion induced by two pore-forming toxins, the *Clostridium perfringens* epsilon-toxin and the *Aeromonas hydrophila* aerolysin toxin, is associated with decreased mitochondrial membrane potential and opening of the mitochondrial permeability transition pore. To gain further insight into the toxin-induced metabolic changes contributing to necrosis and depletion of ATP, we analyzed the biochemical profiles of 251 distinct compounds by GC/MS or LC/MS/MS following exposure of a human kidney cell line to the epsilon-toxin. As expected, numerous biochemicals were seen to increase or decrease in response to epsilon-toxin. However, the pattern of these changes was consistent with the toxin-induced disruption of major energy-producing pathways in the cell including disruptions to the beta-oxidation of lipids. In particular, treatment with epsilon-toxin led to decreased levels of key coenzymes required for energy production including carnitine, NAD (and NADH), and coenzyme A. Independent biochemical assays confirmed that epsilon-toxin and aerolysin induced the rapid decrease of these coenzymes or their synthetic precursors. Incubation of cells with NADH or carnitine-enriched medium helped protect cells from toxin-induced ATP depletion and cell death. Collectively, these results demonstrate that members of the aerolysin family of pore-forming toxins lead to decreased levels of essential coenzymes required for energy production. The resulting loss of energy substrates is expected to contribute to dissipation of the mitochondrial membrane potential, opening of the mitochondrial permeability transition pore, and ultimately cell death.

Introduction

Greater than 25 percent of all bacterial protein toxins belong to the group of pore-forming toxins, the largest category of bacterial virulence factors [1]. Representatives may be found in both Gram-positive and –negative bacteria, and related proteins may be found in diverse eukaryotic species[2–4]. For example, the *Clostridium perfringens* epsilon-toxin is structurally similar to other pore-forming toxins, including the *C. perfringens* enterotoxin, *C. septicum* α-toxin, *Aeromonas hydrophila* aerolysin, and the *Laetiporus sulphureus* LslA hemolytic lectin [2, 5–7]. Bioinformatics and structure predictions suggest related proteins are found in bacteria, fungi, plants, invertebrates, and fish [4]. Thus, these toxins are models for a broad

†Electronic Supplementary Information (ESI) available: [Table S1]. See DOI: 10.1039/b000000x/

Correspondence to: Mark S. McClain, mark.mcclain@vanderbilt.edu.

[b]These authors contributed equally to this work

family of proteins. At first glance, the action of these toxins appears simple: the toxins form unregulated pores in the plasma membrane of sensitive cells, leading to deregulated ion homeostasis, and ultimately cell death. However, recent studies indicate that the interactions between pore-forming toxins and host cells are more complex. Studies exploring the cytotoxic activities of different pore-forming toxins suggest that host factors (beyond cell-surface receptors) also contribute to toxin-induced cytotoxicity [8–11].

Studies have demonstrated that a variety of pore-forming toxins induce cell death through programmed necrosis, a process widely associated with ischemia/reperfusion injury and neuronal excitotoxicity[12–14]. Like apoptosis, programmed necrosis is the result of a concerted series of intracellular signalling and biochemical events leading to cell death [15, 16]. Whereas apoptosis is characterized by activation of executioner caspases (e.g., caspases 3, 6 and 7) and minimal decreases in ATP levels, programmed necrosis is characterized as being insensitive to caspase inhibitors and by rapid depletion of cellular ATP [17, 18]. Cellular ATP levels appear to be an indicator, if not a determinant of whether cell death proceeds via apoptosis or necrosis.

It is widely understood that mitochondria play an important role in cell death, and evidence from multiple studies suggests that depletion of ATP by pore-forming toxins correlates with disruptions to mitochondrial function [12, 19–21]. Key indicators of mitochondrial function include the maintenance of an electrochemical potential across the inner mitochondrial membrane, maintenance of the MPTP in a closed state, and availability of energy-producing substrates. However, unambiguous causal relationships between nutrient availability, MPTP opening, and mitochondrial membrane potential have not been clearly established in response to diverse cellular stresses (including ischemia/reperfusion, excitotoxicity, and other stresses inducing programmed necrosis). For example, mitochondria utilize oxidizable substrates and coenzymes such as NAD^+ (and its reduced form, NADH) to produce a membrane potential in the form of a proton gradient across the mitochondrial inner membrane. Nutrient limitation or NAD^+ depletion have been shown to lead to reduced glucose carbon flux to the mitochondrial TCA cycle which leads to a decline in mitochondrial membrane potential and MPTP opening [22–27]. In contrast, MPTP opening also has been reported to precede NAD^+ depletion [28]. Furthermore, opening of the MPTP and depolarization of the mitochondrial membrane can cause ATP synthase to begin hydrolysing, rather than producing, ATP [29].

In the present study, we characterize the effects of the poreforming toxins epsilon-toxin and aerolysin on cellular metabolism using a human kidney cell line, a comprehensive metabolomics platform, and assays for specific metabolites. We identify reproducible alterations in coenzyme (NAD^+, NADH, CoA, and carnitine) levels induced by the epsilon-toxin and show that changes in these coenzymes or in their synthetic precursors are recapitulated by aerolysin. Supplementation of culture medium with NADH or carnitine is partially protective against the pore-forming toxins, providing evidence that toxin-induced decline in coenzyme levels contributes to the loss of ATP and ultimately cell death.

Results

Aerolysin-family toxins lead to depleted ATP levels in cells

In initial experiments aimed at characterizing the cellular response to epsilon-toxin and aerolysin, we measured cytotoxicity in ACHN cells exposed to each toxin for 1.5 or 16 hours. Each toxin exhibited dose-dependent cytotoxicity (Fig. 1A). A dose of each toxin sufficient for killing >90% of the monolayer in 16 hours was also sufficient to kill greater than 70% of the cells in 90 minutes (Fig. 1B). As an indicator of plasma membrane integrity

(and an additional indicator of cell death), we monitored the release of LDH in response to the toxins (Fig. 1C).

Cellular ATP levels are a distinguishing feature differentiating apoptosis from programmed necrosis. Cells induced to undergo apoptosis retain cellular ATP levels. In contrast, cells exposed to epsilon-toxin or aerolysin exhibit a rapid depletion of cellular ATP, consistent with programmed necrosis (Fig. 2A). The ATP-producing capacity of mitochondria relies on the membrane potential across the inner mitochondrial membrane. To further explore the effects of pore-forming toxins on mitochondrial function, we monitored changes in mitochondrial membrane potential using a potential-sensitive fluorescent dye. Untreated cells maintain a potential across the mitochondrial membrane, whereas cells treated with the proton ionophore CCCP exhibit a decrease in the fluorescent signal indicating a decrease in the mitochondrial membrane potential (Fig. 2B). Cells treated with either the *C. perfringens* epsilon-toxin or with *A. hydrophila* aerolysin also exhibit a decrease in the fluorescent signal, indicating that the toxins dissipate the mitochondrial membrane potential (Fig. 2B). Cells pre-treated with cyclosporine A, an inhibitor of the MPTP, were able to partially maintain ATP levels following toxin treatment compared to cells that were not treated with cyclosporine A (Fig. 2C). These results indicate that the depletion of ATP induced by epsilon-toxin or aerolysin coincides with decreased mitochondrial membrane potential and opening of the MPTP, indicating that the toxins disrupt mitochondrial activity.

Aerolysin-family toxins disrupt the energy producing capacity of cells

To determine what changes accompany the depletion of ATP, we performed a detailed metabolomics study of untreated control cells as well as cells treated with either heat-inactivated epsilon-toxin or active epsilon-toxin. Samples were prepared following 30 or 60 minutes of treatment. For comparison, the 251 metabolites analyzed were categorized as belonging to one of 7 pathways, including 47 sub-pathways, and fold-changes were determined for each pairwise treatment combination (i.e., heat-inactivated vs. untreated control, toxin-treated vs. untreated control, and toxin-treated vs. heat-inactivated). Few changes were detected between cells treated with heat-inactivated toxin and the untreated control cells. In contrast, numerous significant changes were detected between cells treated with active toxin and either of the other treatment groups (Fig. 3 and Table S1). The changes induced by the active epsilon-toxin included increases and decreases in a variety of metabolites (Figure 3). Compounds that appeared to increase in reposnse to toxin treatment included several amino acids (Arg, His, Ile, Leu, Met, and Val), as well as essential, medium- and long-chain fatty acids, and sphingolipids. Compounds that appeared to decrease in response to the toxin included amino acids (Asp, Cys, Glu, and Pro), neurotransmitters (gamma-aminobutyrate, N-acetylaspartate and N-acetyl-aspartylglutamate), TCA cycle intermediates, carnitine and acylcarnitines, and other cofactors and vitamins (including NAD^+, NADH, pantothenate, CoA). Although beyond the scope of the present study, toxin-induced changes in the levels of neurotransmitters might help explain epsilon-toxin's neurological effects[30–32].

Overall, however, results were consistent with toxin-induced perturbation of major energy-producing pathways in the cell. The reactions of the TCA cycle occur within the mitochondrial matrix in eukaryotic cells and are important to the generation of energy from carbohydrates, proteins and lipids. Compared to untreated control cells, epsilon-toxin-treated cells exhibited decreased levels of TCA cycle intermediates such as citrate, fumarate and malate (Table S1). In contrast, epsilon-toxin-treated cells exhibited increased levels of

[†]Electronic Supplementary Information (ESI) available: [Table S1]. See DOI: 10.1039/b000000x/

pyruvate, a major entry point into the TCA cycle (Table S1), as well as increased levels of intermediates of the non-oxidative phase of the pentose-phosphate pathway (Table S1).

Evidence of toxin-induced perturbation of energy producing pathways was also observed in metabolites related to the beta-oxidation of lipids. Compared to untreated control cells, epsilon-toxin-treated cells exhibited decreased levels of beta-oxidation intermediates such as fatty-acyl-carnitines and significantly increased levels of long-chain fatty acids, the substrates of beta-oxidation (Table 1). Additionally, when the beta-oxidation of free fatty acids is impaired, cells may switch to omega-oxidation. A consequence of omega-oxidation is the accumulation of dicarboxylic acids such as azelate (Table 1) [33].

Cells treated with aerolysin-family toxins exhibit reduced CoA levels

The metabolomics analysis revealed that epsilon-toxin treated cells exhibit decreased levels of pantothenate, an essential nutrient used as the precursor to CoA, as well as synthetic intermediates such as cysteine, 3'-dephosphoCoA, and CoA itself (Table 1). To determine whether another member of the aerolysin-family might induce a similar response (and as independent confirmation of the metabolomics analysis), we measured cellular pantothenate levels in untreated cells as well as in cells treated with either epsilon-toxin or aerolysin. *Lactobacillus plantarum* ATCC 8014 is a pantothenate auxotroph. The extent of growth of this *L. plantarum* strain in a defined medium is dependent on the pantothenate concentration[34]. To assess the toxin-dependent decrease in pantothenate levels, *L. plantarum* was grown in assay medium supplemented with either pantothenate or with cell lysates prepared from toxin-treated cells. Both toxins induced the rapid decline of cellular pantothenate (Fig. 4A). Conversely, a similar analysis of the culture medium indicated that the extracellular levels of pantothenate increased over time in response to the toxins (Fig. 4A).

Cells treated with aerolysin-family toxins exhibit reduced carnitine levels

Like CoA, carnitine is a coenzyme required for energy production through beta-oxidation of lipids. The metabolomics analysis revealed that epsilon-toxin treated cells exhibit decreased carnitine levels (Table 1). To confirm and extend these results, we measured carnitine levels in cells treated with either epsilon-toxin or aerolysin. The extent of growth of *Candida pintolopesii* ATCC26014 in a defined medium is dependent on the carnitine concentration[35]. To assess the toxin-dependent depletion of carnitine from cells, *C. pintolopesii* was grown in assay medium supplemented with either carnitine or with cell lysates prepared from toxin-treated cells. Both toxins induced a rapid decrease in cellular carnitine levels (Fig. 4B). Similar results were obtained using an enzymatic assay for carnitine (data not shown). Conversely, a similar analysis of the culture medium indicated that the extracellular levels of carnitine increased over time in response to the toxins (Fig. 4B).

Cells treated with aerolysin-family toxins exhibit reduced NAD^+ and NADH levels

Like CoA and carnitine, NAD^+ (and its reduced form NADH) is a coenzyme utilized for energy production. The metabolomics analysis revealed that epsilon-toxin treated cells exhibit decreases in NAD^+ and NADH levels, as well as nicotinic acid adenine dinucleotide ($NAAD^+$, a precursor for NAD^+ synthesis via the *de novo* pathway) (Table 1). To confirm and extend these results, we measured NAD^+ and NADH levels in cells treated with either epsilon-toxin or aerolysin. Results indicated that both toxins induced a decrease in NAD^+ and NADH in cells (Fig. 4C).

NADH and carnitine protect against ATP depletion and cell death

The toxin-induced declines in NAD^+ (and NADH), carnitine, and pantothenate levels led us to investigate whether media supplementation with these metabolites could protect against toxin-induced ATP depletion. ACHN cells were incubated in a balanced salt solution with or without the addition of 5 mM NADH, carnitine, or pantothenate for 1 hour prior to addition of either epsilon-toxin or aerolysin. Analysis of cellular ATP content indicated that supplementation with either NADH or carnitine partially protected cells from the toxin-induced ATP loss (Fig. 5A and B). Pantothenate provided no protection against ATP loss induced by either toxin (data not shown).

To further explore the protective effect of carnitine, we investigated whether media supplementation with carnitine could protect against toxin-induced release of LDH, a marker for plasma membrane disruption and cell death (NADH supplementation interfered with the assay used to monitor LDH release and therefore was not tested). ACHN cells were incubated in a balanced salt solution with or without the addition of 5 mM carnitine for 1 hour prior to addition of either epsilon-toxin or aerolysin. Enzymatic analysis of LDH release indicated that supplementation with carnitine protected cells from the toxins as evidenced by an increase in the mean time to death (Fig. 5C).

Discussion

Pore-forming toxins such as epsilon-toxin have been known to disrupt ion homeostasis in cells. Toxin-induced changes in Na^+, K^+, Cl^-, and Ca^{2+} have all been studied and likely contribute to cytotoxicity [36, 37]. Less well understood are the toxin-induced changes in metabolites and how such changes might also contribute to ATP depletion and cell death. The analyses detailed in the current study elucidate toxin-induced changes in metabolites indicative of cell death, including numerous changes demonstrating that members of the aerolysin family of pore-forming toxins induce disruption of mitochondrial activity.

In particular, the metabolic analyses demonstrate that the toxins induce decreased levels of essential coenzymes, including CoA (and its precursor, pantothenate), NAD^+ and NADH, and carnitine. Results of the present study suggest that pantothenate (an essential precursor to CoA) and carnitine (and likely other metabolites) leak from the cell in response to the pore-forming toxins. Though we cannot, at present, determine whether the molecules are leaking through pores formed by the toxins or through other cellular channels, previous studies have demonstrated that the pores formed by the toxins are of sufficient size to allow the passage of pantothenate (219 Da) and carnitine (161 Da) [38–40]. Specifically, pores formed by epsilon toxin are approximately 0.5 nm in diameter and allow passage of molecules up to 500 Da in size, whereas pores formed by aerolysin are approximately 1.9 nm in diameter and allow passage of molecules up to 3550 Da in size [38–40]. We also were not able to determine whether NAD^+ or NADH leaked from the cell, perhaps due to limited sensitivity of the enzymatic assay used to detect NAD^+ and NADH. Previous studies have attributed NAD^+ depletion during necrotic cell death to activation of PARP [41–43]. However, we were unable to detect PARP activation in response to the toxins (data not shown) and recent studies have demonstrated that depletion of cytosolic NAD^+ is sufficient, in the absence of PARP activation, to impair mitochondrial activity and promote cell death [26]. Supplementation with NADH or with carnitine mitigated the effects of the pore-forming toxins, protecting cells from ATP depletion and prolonging time to death. Presumably, the added carnitine and NADH entered cells either through toxin-induced pores or through natural internalization processes such as specific transporters (in the case of carnitine) or Cx43 or P2×7 channels (in the case of NADH) [26, 44–47]. These results demonstrate that the toxin-induced depletion of NAD^+ (or NADH) and carnitine contributes to the cytotoxic effects of the pore-forming toxins. In contrast, supplementation with pantothenate did not

protect against ATP decline or LDH release. One possible explanation for this latter result would be if one or more enzymes needed to convert pantothenate to CoA also leaked from the cell

Though unambiguous causal relationships between nutrient availability, MPTP opening, and mitochondrial membrane potential have not been clearly established in response to diverse cellular stresses, the toxin-induced declines in carnitine and NAD^+ (and NADH) described in the current study contribute to toxin-induced ATP depletion and cell death. One mechanism by which the toxin-induced coenzyme depletion likely contributes is by limiting the availability of substrates used by the cell to produce ATP. For example, carnitine is required for transport of fatty acids into the mitochondrial matrix via the carnitine/acylcarnitine shuttle. Once inside the mitochondrial matrix, the lipids are broken down through β-oxidation, generating acetate utilized in the TCA cycle for the generation of ATP. Similarly, toxin-induced declines in NAD^+ and NADH could limit ATP production. The energy released by the oxidation of glucose or fatty acids is transferred to NAD^+ by reduction to NADH during the TCA cycle and lipid beta-oxidation. The NADH is then oxidized by the electron transport chain, which pumps protons across the mitochondrial membrane and generates ATP through oxidative phosphorylation.

The toxin-induced coenzyme depletion may also contribute to disruption of mitochondrial activity by inducing a decrease in the mitochondrial membrane potential and to opening of the MPTP. For example, protons produced by the oxidation of NADH to NAD^+ generate the electrochemical gradient across the inner mitochondrial membrane. Similarly, inhibition of beta-oxidation as a consequence of decreased carnitine depletion is expected to lead to the accumulation of long-chain fatty acids (as shown in Table 1). Previous studies have demonstrated that long-chain fatty acids can induce the opening of the MPTP [48, 49]. In contrast, opening of the MPTP in response to fatty acids or a variety of other chemicals can be inhibited by the addition of carnitine [50–52]. MPTP opening, in addition to negatively impacting ATP production, also is associated with release of cell death effectors such as AIF [53–55]. In multiple experimental models, including the cytotoxicity of epsilon-toxin, AIF release from mitochondria has been implicated in cell death [12, 56, 57].

Results of the present study expand our understanding of important molecular changes that occur within cells in response to members of the aerolysin-family of pore-forming toxins (and perhaps other pore-forming toxins such as the cholesterol-dependent cytolysins and *Staphylococcus aureus* alpha hemolysin). Toxin-induced changes in cellular ion homeostasis have previously been shown to stimulate a variety of signalling cascades including pathways believed to stimulate membrane repair and to reduce energy consumption [58]. These efforts by the cell to protect against the toxins, however, may be aggravated by the toxin-induced ATP decline brought on (at least in part) by the decreased levels of essential coenzymes. Additional experiments, beyond the scope of the present study, may determine whether carnitine or NADH supplementation provide a therapeutic benefit in treating animals exposed to these or other toxins.

Experimental

Cell Culture

ACHN cells were obtained from ATCC. For routine culture, cells were grown in MEM supplemented with 10% serum (Fetal Clone III, HyClone). Unless otherwise indicated, incubations of cells with toxins were performed in phenol red-free Leibovitz L-15 medium supplemented with 10% serum (Fetal Clone III, HyClone).

Toxins

C. perfringens epsilon-toxin was expressed and purified as a recombinant protein in *E. coli* as described [8, 59, 60]. The identification of the epsilon-prototoxin in the purified sample was confirmed by immunoblotting with epsilon-toxin-specific monoclonal antibody. Purity was monitored by SDS-PAGE and silver staining. Protein concentrations were determined using micro-BCA (Pierce). Conversion of the epsilon-prototoxin to the active epsilon-toxin was achieved by treating purified prototoxin with trypsin [8, 59, 60]. Conversion of the epsilon-prototoxin to epsilon-toxin was assessed based on SDS-PAGE and immunoblotting with anti-epsilon-toxin antibodies. Heat-inactivation of the epsilon-toxin was carried out by heating the toxin at 60°C for 30 minutes, a treatment sufficient to render the toxin indistinguishable from buffer alone when incubated with ACHN cells for 16 hours followed by treatment with CellTiter Blue (Promega) (data not shown).

Pro-aerolysin was obtained from Protox Biotech (Victoria, BC, Canada) and is converted to the active aerolysin toxin by cell-surface proteases [61].

Cytotoxicity assays

CellTiter Blue (Promega) was used as a general measure of cellular metabolic capacity. Cellular ATP levels were determined using a luciferase-based assay according to the manufacturer's instructions (ATPLite 1-Step, Perkin Elmer). Release of LDH from cells was monitored using the CytoTox-ONE Homogeneous Membrane Integrity Assay (Promega). Fluorescence or luminescence was monitored using a BioTek Flx800 plate reader.

Mitochondrial membrane potential

Changes in the mitochondrial membrane potential were detected using Mito-ID membrane potential cytotoxicity kit (ENZO Life Sciences, Farmingdale, NY). ACHN cells were pre-loaded with the potential-sensitive dye at 37°C for 30 minutes. The fluorescent signal (Ex=485 nm/Em=590 nm) was monitored over time using a BioTek Flx800 plate reader. The fluorescent signal was monitored at 5 minute intervals for a period of 90 minutes after toxin addition. For each dye-loaded well, the $\Delta F/F_0$ value was generated at each timepoint (*i.e.*, the fractional change in fluorescence over basal). The $\Delta F/F_0$ values for wells to which only buffer was added were averaged at each timepoint. These averaged values were then subtracted from the corresponding values in all wells. This compensated for fluorescence changes due to dye bleaching, and other artifacts. The mean of the value was then determined across all wells to which the same treatment was applied [62].

Metabolomics

Metabolic changes in ACHN cells following exposure to *C. perfringens* epsilon-toxin were profiled. ACHN cells are a human renal cell adenocarcinoma line obtained from the American Type Culture Collection. The epsilon-toxin was expressed as a recombinant protein in *E. coli* HMS174 (DE3) and purified by ion-exchange and metal-affinity chromatography as described [8, 59, 60]. The purified toxin was activated by treating with trypsin as described [8, 59, 60]. ACHN cells were cultured as monolayers on 25 cm^2 flasks (Cellstar, Greiner Bio-One) in phenol red-free Leibovitz L-15 medium (Invitrogen) supplemented with 10% serum (Hyclone FetalClone III, Thermo) and incubated at 37°C in ambient air. Cells were seeded into the flasks 20 hours before the start of the treatment. Treatment consisted of replacing the medium overlying the cells with L-15 medium supplemented with 10% serum, with the same medium supplemented with 500 nM heat-inactivated epsilon-toxin, or with the same medium supplemented with 500 nM active epsilon-toxin. Five replicates were prepared for each treatment. Samples were harvested 30 or 60 minutes after the start of the treatment. Monolayers were washed twice in PBS, and

cells were dislodged from the dishes with trypsin. The trypsinized cells were washed twice in PBS supplemented with a protease inhibitor cocktail (Complete Mini, Boerhinger), and resuspended in a minimal residual volume of PBS. An aliquot of each sample was counted on a hemocytometer; the mean cell density was 2.1×10^5 cells per cm^2. All samples were heated to 60°C for 30 minutes to inactivate epsilon-toxin [a treatment sufficient to render the toxin indistinguishable from buffer alone when incubated with ACHN cells for 16 hours followed by treatment with CellTiter Blue (Promega)], and then frozen at −80°C. Samples were shipped on dry ice to Metabolon, Inc. for analysis as described previously [63, 64].

Specific metabolite assays

Cellular NAD (NAD^+ and NADH) levels were determined using an enzyme recycling assay (Abcam). Fluorescence was monitored using a BioTek Flx800 plate reader. Changes in pantothenate and carnitine were determined using sensitive microbiological assays, with minor modifications [34 35]. ACHN cells were incubated in a balanced salt solution (130 mM NaCl, 5 mM KCl, 2 mM $MgCl_2$, 1 mM $CaCl_2$, and 10 mM HEPES, pH 7.3) in the presence or absence of toxins then washed twice with PBS. Cell lysates were prepared with M-PER according to manufacturer's instructions (Pierce). For monitoring changes in pantothenate, lysates (or tissue culture supernatants) were diluted into Difco Pantothenate Assay Medium and inoculated with *L. plantarum* ATCC 8014. Cultures were shaken at 37°C for 16 hours, and the optical density at 600 nm was determined using a plate reader (Bio-Rad). For monitoring changes in carnitine, lysates (or tissue culture supernatants) were diluted into carnitine-free assay medium and inoculated with *C. pintolopesii* ATCC 26014. Cultures were shaken at 37°C for 30 hours, and the optical density at 540 nm was determined using a plate reader (Bio-Rad). Results were compared to cultures prepared in carnitine-free assay medium supplemented with known concentrations of carnitine.

Acknowledgments

This study was supported by National Institutes of Health grant R01-AI079123 to MSM. The content is solely the responsibility of the authors and does not necessarily represent the official views of the National Institute of Allergy and Infectious Diseases or the National Institutes of Health. The funding agency had no role in study design, data collection and analysis, decision to publish, or preparation of the manuscript.

Abbreviations

CoA	coenzyme A
MPTP	mitochondrial permeability transition pore
CCCP	carbonyl cyanide 3-chlorophenylhydrazone
TCA	tricarboxylic acid
LDH	lactate dehydrogenase
PARP	poly (ADP-ribose) polymerase
AIF	apoptosis inducing factor

References

1. The Comprehensive Sourcebook of Bacterial Protein Toxins. Third Edition edn. Amsterdam: Elsevier; 2006.
2. Mancheno JM, Tateno H, Goldstein IJ, Martinez-Ripoll M, Hermoso JA. J. Biol. Chem. 2005; 280:17251–17259. [PubMed: 15687495]
3. Mancheno JM, Tateno H, Sher D, Goldstein IJ. Adv. Exp. Med. Biol. 2010; 677:67–80. [PubMed: 20687481]

4. Szczesny P, Iacovache I, Muszewska A, Ginalski K, vanderGoot FG, Grynberg M. PLoS One. 2011; 6:e20349. [PubMed: 21687664]
5. Cole AR, Gibert M, Popoff M, Moss DS, Titball RW, Basak AK. Nat Struct Mol Biol. 2004; 11:797–798. [PubMed: 15258571]
6. Parker MW, Buckley JT, Postma JP, Tucker AD, Leonard K, Pattus F, Tsernoglou D. Nature. 1994; 367:292–295. [PubMed: 7510043]
7. Briggs DC, Naylor CE, Smedley JG Iii, Lukoyanova N, Robertson S, Moss DS, McClane BA, Basak AK. J. Mol. Biol. 2011; 413:138–149. [PubMed: 21839091]
8. Ivie SE, Fennessey CM, Sheng J, Rubin DH, McClain MS. PLoS One. 2011; 6:e17787. [PubMed: 21412435]
9. Skals M, Jorgensen NR, Leipziger J, Praetorius HA. Proc. Natl. Acad. Sci. U. S. A. 2009; 106:4030–4035. [PubMed: 19225107]
10. Soletti RC, Alves T, Vernal J, Terenzi H, Anderluh G, Borges HL, Gabilan NH, Moura-Neto V. Anticancer Res. 30:1209–1215. [PubMed: 20530430]
11. Zhang X, Candas M, Griko NB, Taussig R, Bulla LA Jr. Proc. Natl. Acad. Sci. U. S. A. 2006; 103:9897–9902. [PubMed: 16788061]
12. Chassin C, Bens M, de Barry J, Courjaret R, Bossu JL, Cluzeaud F, Ben Mkaddem S, Gibert M, Poulain B, Popoff MR, Vandewalle AJ. Am J Physiol Renal Physiol. 2007; 293:F9927–F9937.
13. Essmann F, Bantel H, Totzke G, Engels IH, Sinha B, Schulze-Osthoff K, Janicke RU. Cell Death Differ. 2003; 10:1260–1272. [PubMed: 12894214]
14. Radin JN, Gonzalez-Rivera C, Ivie SE, McClain MS, Cover TL. Infect. Immun. 2011; 79:2535–2543. [PubMed: 21482684]
15. Zong WX, Thompson CB. Genes Dev. 2006; 20:1–15. [PubMed: 16391229]
16. Yamashima T. Cell Calcium. 2004; 36:285–293. [PubMed: 15261484]
17. McConkey DJ. Toxicol. Lett. 1998; 99:157–168. [PubMed: 9862281]
18. Kroemer G, Dallaporta B, Resche-Rigon M. Annu. Rev. Physiol. 1998; 60:619–642. [PubMed: 9558479]
19. Kennedy CL, Smith DJ, Lyras D, Chakravorty A, Rood JI. PLoS Pathog. 2009; 5:1000516.
20. Knapp O, Maier E, Mkaddem SB, Benz R, Bens M, Chenal A, Geny B, Vandewalle A, Popoff MR. Toxicon. 2010; 55:61–72. [PubMed: 19632260]
21. Zitzer A, Wassenaar TM, Walev I, Bhakdi S. Infect. Immun. 1997; 65:1293–1298. [PubMed: 9119464]
22. Vander Heiden MG, Plas DR, Rathmell JC, Fox CJ, Harris MH, Thompson CB. Mol. Cell. Biol. 2001; 21:5899–5912. [PubMed: 11486029]
23. Kan O, Baldwin SA, Whetton AD. The Journal of Experimental Medicine. 1994; 180:917–923. [PubMed: 8064240]
24. Zong W-X, Ditsworth D, Bauer DE, Wang Z-Q, Thompson CB. Genes, Development. 2004; 18:1272–1282. [PubMed: 15145826]
25. Ying W, Alano CC, Garnier P, Swanson RA. J. Neurosci. Res. 2005; 79:216–223. [PubMed: 15562437]
26. Alano CC, Garnier P, Ying W, Higashi Y, Kauppinen TM, Swanson RA. The Journal of Neuroscience. 2010; 30:2967–2978. [PubMed: 20181594]
27. Doczi J, Turiák L, Vajda S, Mándi M, Töröcsik B, Gerencser AA, Kiss G, Konràd C, Adam-Vizi V, Chinopoulos C. J. Biol. Chem. 2011; 286:6345–6353. [PubMed: 21173147]
28. Di Lisa F, Menabò R, Canton M, Barile M, Bernardi P. J. Biol. Chem. 2001; 276:2571–2575. [PubMed: 11073947]
29. Stavrovskaya IG, Kristal BS. Free Radic. Biol. Med. 2005; 38:687–697. [PubMed: 15721979]
30. Fernandez-Miyakawa ME, Sayeed S, Fisher DJ, Poon R, Adams V, Rood JI, McClane BA, Saputo J, Uzal FA. Infect. Immun. 2007; 75:4282–4288. [PubMed: 17562765]
31. Uzal FA, Kelly WR. J. Comp. Pathol. 1997; 116:63–71. [PubMed: 9076601]
32. Uzal FA, Kelly WR, Morris WE, Bermudez J, Baison M. J. Vet. Diagn. Invest. 2004; 16:403–411. [PubMed: 15460322]

33. Mortensen PB. Dan. Med. Bull. 1984; 31:121–145. [PubMed: 6426867]
34. Barton-Wright, EC. Practical Methods for the Microbiological Assay of Vitamin B complex and Essential Amino acids. London: Ashe Laboratories; 1946.
35. Travassos LR, Sales CO. Anal. Biochem. 1974; 58:485–499. [PubMed: 4857116]
36. Petit L, Gibert M, Gillet D, Laurent-Winter C, Boquet P, Popoff MR. J. Bacteriol. 1997; 179:6480–6487. [PubMed: 9335299]
37. Petit L, Maier E, Gibert M, Popoff MR, Benz R. J. Biol. Chem. 2001; 276:15736–15740. [PubMed: 11278669]
38. Nestorovich EM, Karginov VA, Bezrukov SM. Biophys. J. 2010; 99:782–789. [PubMed: 20682255]
39. Howard SP, Buckley JT. Biochemistry (Mosc). 1982; 21:1662–1667.
40. Macpherson HL, Bergh Ø, Birkbeck TH. Journal of Fish Diseases. 2012; 35:153–167. [PubMed: 22233514]
41. Di Lisa F, Bernardi P. Cardiovasc. Res. 2006; 70:191–199. [PubMed: 16497286]
42. Ha HC, Snyder SH. Proc. Natl. Acad. Sci. U. S. A. 1999; 96:13978–13982. [PubMed: 10570184]
43. Thiemermann C, Bowes J, Myint FP, Vane JR. Proc. Natl. Acad. Sci. U. S. A. 1997; 94:679–683. [PubMed: 9012844]
44. Tamai I, China K, Sai Y, Kobayashi D, Nezu J, Kawahara E, Tsuji A. Biophys. Biochim. Acta. 2001; 1512:273–284.
45. Lu H, Burns D, Garnier P, Wei G, Zhu K, Ying W. Biochem. Biophys. Res. Commun. 2007; 362:946–950. [PubMed: 17803959]
46. Bruzzone S, Guida L, Zocchi E, Franco L, De Flora A. The FASEB Journal. 2000; 15:10–12.
47. Wang S, Xing Z, Vosler PS, Yin H, Li W, Zhang F, Signore AP, Stetler RA, Gao Y, Chen J. Stroke. 2008; 39:2587–2595. [PubMed: 18617666]
48. Wieckowski MR, Brdiczka D, Wojtczak L. FEBS Lett. 2000; 484:61–64. [PubMed: 11068032]
49. Wieckowski MR, Wojtczak L. FEBS Lett. 1998; 423:339–342. [PubMed: 9515735]
50. Furuno T, Kanno T, Arita K, Asami M, Utsumi T, Doi Y, Inoue M, Utsumi K. Biochem. Pharmacol. 2001; 62:1037–1046. [PubMed: 11597572]
51. Kashiwagi A, Kanno T, Arita K, Ishisaka R, Utsumi T, Utsumi K. Comp. Biochem. Physiol. B. Biochem. Mol. Biol. 2001; 130:411–418. [PubMed: 11567904]
52. Pastorino JG, Snyder JW, Serroni A, Hoek JB, Farber JL. J. Biol. Chem. 1993; 268:13791–13798. [PubMed: 8314748]
53. Petit PX, Goubern M, Diolez P, Susin SA, Zamzami N, Kroemer G. FEBS Lett. 1998; 426:111–116. [PubMed: 9598989]
54. Alano CC, Ying W, Swanson RA. J. Biol. Chem. 2004; 279:18895–18902. [PubMed: 14960594]
55. Polster BM, Basañez G, Etxebarria A, Hardwick JM, Nicholls DG. J. Biol. Chem. 2005; 280:6447–6454. [PubMed: 15590628]
56. Vega-Manriquez X, Lopez-Vidal Y, Moran J, Adams LG, Gutierrez-Pabello JA. Infect. Immun. 2007; 75:1223–1228. [PubMed: 17158896]
57. Wang H, Yu SW, Koh DW, Lew J, Coombs C, Bowers W, Federoff HJ, Poirier GG, Dawson TM, Dawson VL. J. Neurosci. 2004; 24:10963–10973. [PubMed: 15574746]
58. Gonzalez MR, Bischofberger M, Freche B, Ho S, Parton RG, van der Goot FG. Cell Microbiol. 2011; 13:1026–1043. [PubMed: 21518219]
59. Lewis M, Weaver CD, McClain MS. Toxins (Basel). 2010; 2:1825–1847. [PubMed: 20721308]
60. Pelish TM, McClain MS. J. Biol. Chem. 2009; 284:29446–29453. [PubMed: 19720828]
61. Abrami L, Fivaz M, Decroly E, Seidah NG, Jean F, Thomas G, Leppla SH, Buckley JT, van der Goot FG. J. Biol. Chem. 1998; 273:32656–32661. [PubMed: 9830006]
62. Simpson PB, Woollacott AJ, Hill RG, Seabrook GR. Eur. J. Pharmacol. 2000; 392:1–9. [PubMed: 10748265]
63. Reitman ZJ, Jin G, Karoly ED, Spasojevic I, Yang J, Kinzler KW, He Y, Bigner DD, Vogelstein B, Yan H. Proceedings of the National Academy of Sciences. 2011; 108:3270–3275.

64. Evans AM, DeHaven CD, Barrett T, Mitchell M, Milgram E. Anal. Chem. 2009; 81:6656–6667. [PubMed: 19624122]

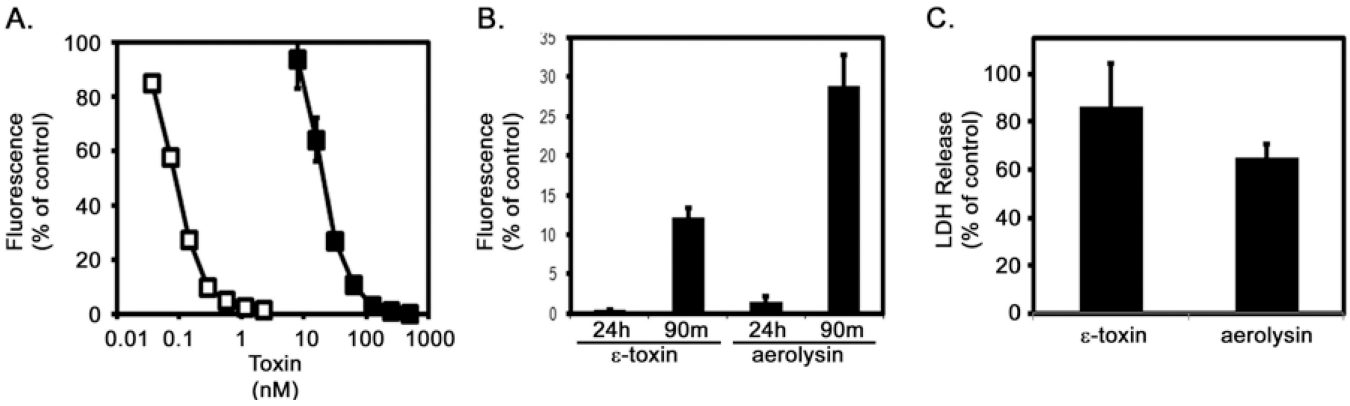

Fig. 1.

Cytotoxicity. A. ACHN cells were incubated at 37°C for 24 hours with serial dilutions of purified epsilon-toxin (■, 7.8 to 500 nM) or aerolysin (□, 0.04 to 2.5 nM). Cytotoxicity was assessed by addition of CellTiter Blue reagent to detect metabolically active cells. Results were normalized to the fluorescent signal from untreated cells (100%) and cells treated with 1% Triton (0%). Results represent the mean and standard deviation of quadruplicate samples. B. ACHN cells were incubated at 37°C for 90 minutes or 24 hours with 500 nM epsilon-toxin or 2.5 nM aerolysin. Cytotoxicity was assessed by addition of CellTiter Blue reagent to detect metabolically active cells. Results were normalized to the fluorescent signal from untreated cells (100%) and cells treated with 1% Triton (0%). Results represent the mean and standard deviation of triplicate samples. C. ACHN cells were incubated at 37°C for 90 minutes with 500 nM epsilon-toxin or 2.5 nM aerolysin. Extracellular LDH was measured using the CytoTox-ONE Homogeneous Membrane Integrity Assay (Promega). Results represent the mean and standard deviation of triplicate samples. These experiments were performed at least three times with similar results.

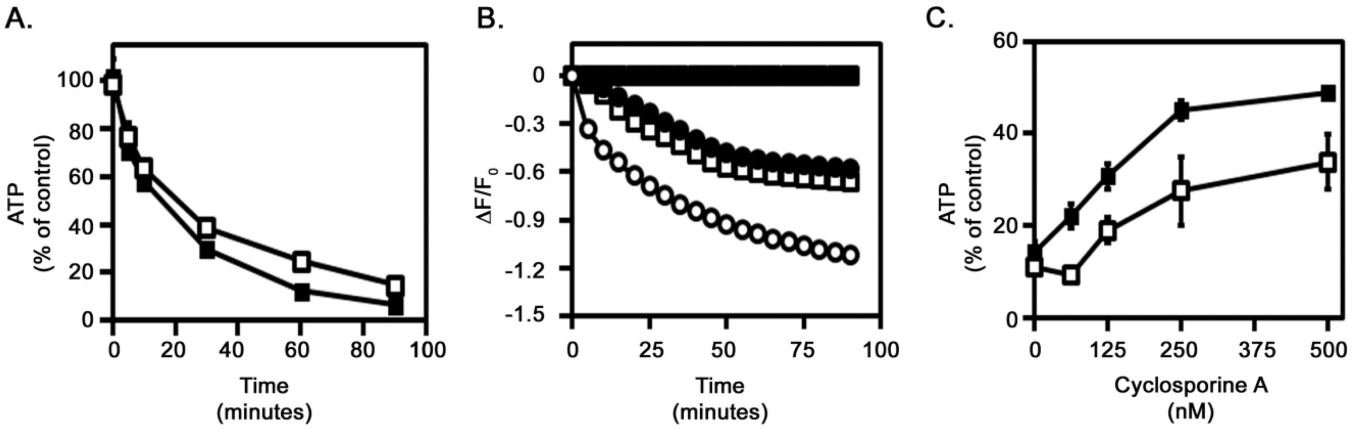

Fig. 2.

Toxin-induced ATP depletion and mitochondrial perturbation. A. ACHN cells were incubated at 37°C for 90 minutes with 500 nM epsilon-toxin (■) or 2.5 nM aerolysin (□). Cellular ATP levels were assessed using ATPLite 1 Step (Perkin Elmer). Results were normalized to the fluorescent signal from untreated cells (100%) and cells treated with 1% Triton (0%). Results represent the mean and standard deviation of triplicate samples. B. ACHN cells were preloaded with a mitochondrial membrane potential-sensitive dye at 37°C for 45 minutes. Cells then were either untreated (■) or treated with 500 nM epsilon-toxin (□), 2.5 nM aerolysin (●), or 500 nM CCCP (○) as a control. The fluorescent signal was monitored at 5 minute intervals for a period of 90 minutes after treatment. Results represent the mean and standard deviation of eight replicate samples; error bars may be too small to be visualised. C. ACHN cells were incubated with serial dilutions of cyclosporine A (62.5 to 500 nM) at 37°C for 60 minutes. Purified epsilon-toxin (■, 500 nM) or aerolysin (□, 2.5 nM) was added and cells were incubated at 37°C for 90 minutes. Cellular ATP levels were assessed using ATPLite 1 Step (Perkin Elmer). Results were normalized to the fluorescent signal from untreated cells (100%) and cells treated with 1% Triton (0%). Results represent the mean and standard deviation of triplicate samples. These experiments were performed at least three times with similar results.

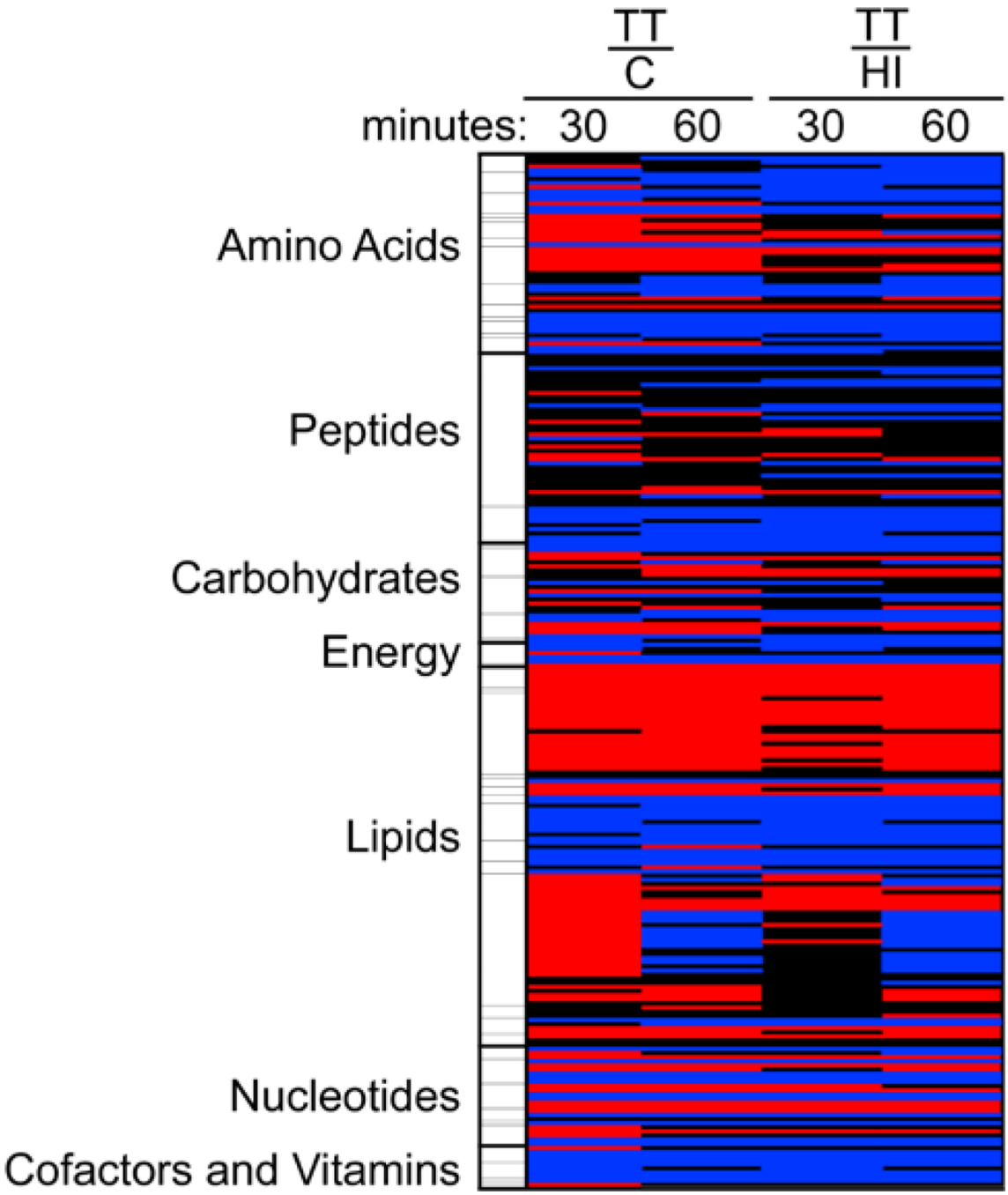

Fig. 3. Heat map of epsilon-toxin-induced metabolic changes

Relative levels of 251 metabolites were determined (as described in Experimental) in untreated control cells (C), cells treated with heat-inactivated epsilon toxin (HI), and cells treated with active epsilon-toxin (TT) for 30 or 60 minutes. The results are presented as the ratio of individual metabolite levels, comparing levels in toxin-treated cells to levels in either control group. For simplicity, metabolites were segregated into 7 pathways as shown. Red: indicates significant difference (ANOVA, $p \leq 0.05$) in metabolite levels between the treatment groups shown, with a mean ratio of > 1. Blue: indicates significant difference (ANOVA, $p \leq 0.05$) between the treatment groups shown, with a mean ratio of < 1. Black:

mean values are not significantly different for that comparison. For additional information, see Table S1.

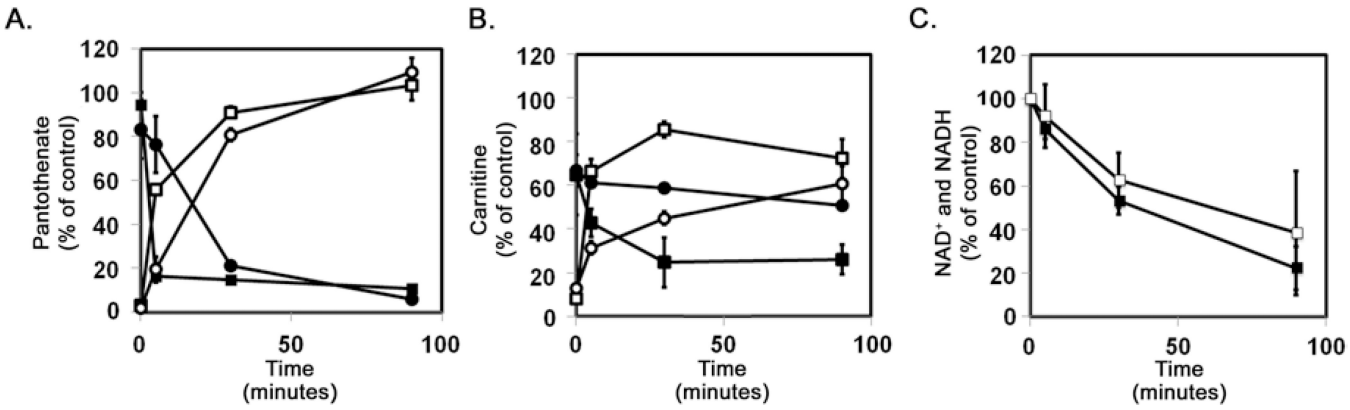

Fig. 4.

Toxin induced decreases in pantothenate, carnitine, and NAD^+ (and NADH). A. ACHN cells were incubated at 37°C for 90 minutes in balanced salt solution with 500 nM ε-toxin or 2.5 nM aerolysin. Culture supernatants were collected, and the cell monolayers then were washed twice in PBS and lysed using M-PER (Pierce). Pantothenate levels in the cell lysates (■, epsilon-toxin; ●, aerolysin) and culture supernatants (□, epsilon-toxin; ○, aerolysin) were assessed using a microbiological assay. The sum of pantothenate levels in the cell lysates and culture supernatants from untreated control cells were determined and the mean value was set at 100%. Results represent the mean and standard deviation of triplicate samples. The microbiological assay was performed at least three times with similar results. B. ACHN cells were incubated at 37°C for 90 minutes in balanced salt solution with 500 nM ε-toxin or 2.5 nM aerolysin. Culture supernatants were collected, and the cell monolayers then were washed twice in PBS and lysed using M-PER (Pierce). Carnitine levels in the cell lysates (■, epsilon-toxin; ●, aerolysin) and culture supernatants (□, epsilon-toxin; ○, aerolysin) were assessed using a microbiological assay. The sum of carnitine levels in the cell lysates and culture supernatants from untreated control cells were determined and the mean value was set at 100%. Results represent the mean and standard deviation of triplicate samples. The microbiological assay was performed at least three times with similar results. C. ACHN cells were incubated at 37°C for 90 minutes in balanced salt solution with 500 nM epsilon-toxin (■) or 2.5 nM aerolysin (□). Cell monolayers then were washed twice in PBS. Total NAD (NAD^+ plus NADH) levels in the cell lysates were assessed using an enzymatic assay. Results were normalized to untreated cells (100%). Results represent the mean and standard deviation of triplicate samples. The enzymatic assay was performed at least three times with similar results.

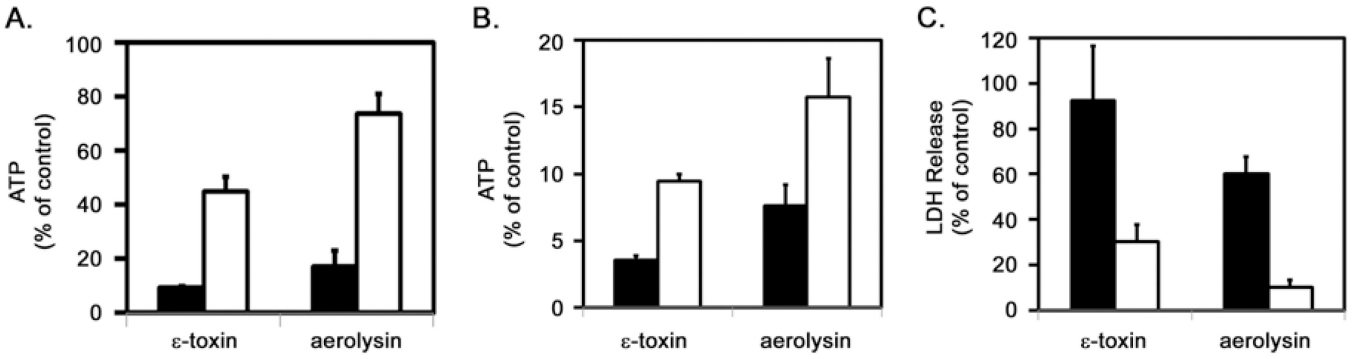

Fig. 5.

ACHN cells were pre-incubated at 37°C for 60 minutes in balanced salt solution (filled bars) or in balanced salt solution supplemented with 5 mM NADH (open bars). Toxins, (500 nM epsilon-toxin or 2.5 nM aerolysin) then were added and the cells were incubated at 37°C for 90 minutes. Cellular ATP levels were assessed using ATPLite 1 Step (Perkin Elmer). Results were normalized to the fluorescent signal from untreated cells (100%) and cells treated with 1% Triton (0%). Results represent the mean and standard deviation of triplicate samples. B and C. ACHN cells were pre-incubated at 37°C for 60 minutes in balanced salt solution (filled bars) or in balanced salt solution supplemented with 5 mM carnitine (open bars). Toxins, (500 nM epsilon-toxin or 2.5 nM aerolysin) then were added and the cells were incubated at 37°C for 90 minutes. Cellular ATP levels were assessed using ATPLite 1 Step (Perkin Elmer) (B) and release of LDH was measured using the CytoTox-ONE Homogeneous Membrane Integrity Assay (Promega) (C). Results represent the mean and standard deviation of triplicate samples. These experiments were performed at least three times with similar results.

Table 1

Selected metabolites

Compound	Epsilon Toxin-Treated / Untreated Control		Epsilon Toxin-Treated / Heat-Inactivated Control	
	30 min[a]	60 min[a]	30 min[a]	60 min[a]
myristate (14:0)	1.71 (< 0.001)	1.71 (< 0.001)	1.38 (< 0.001)	1.52 (< 0.001)
myristoleate (14:1n5)	1.74 (< 0.001)	1.66 (0.002)	1.31 (0.082)	1.7 (0.002)
pentadecanoate (15:0)	1.94 (< 0.001)	1.82 (< 0.001)	1.56 (< 0.001)	1.67 (< 0.001)
palmitate (16:0)	1.78 (< 0.001)	1.74 (< 0.001)	1.52 (< 0.001)	1.5 (< 0.001)
palmitoleate (16:1n7)	1.77 (< 0.001)	1.72 (< 0.001)	1.53 (< 0.001)	1.52 (< 0.001)
margarate (17:0)	2.15 (< 0.001)	2.41 (< 0.001)	1.86 (< 0.001)	1.99 (< 0.001)
10-heptadecenoate (17:1n7)	1.99 (< 0.001)	1.93 (< 0.001)	1.61 (< 0.001)	1.76 (< 0.001)
stearate (18:0)	1.91 (< 0.001)	2.3 (< 0.001)	1.66 (< 0.001)	1.79 (< 0.001)
oleate (18:1n9)	1.51 (0.009)	1.57 (0.002)	1.21 (0.231)	1.36 (0.037)
cis-vaccenate (18:1n7)	1.33 (0.085)	1.67 (< 0.001)	1.11 (0.594)	1.21 (0.232)
nonadecanoate (19:0)	2.37 (< 0.001)	2.51 (< 0.001)	1.7 (0.004)	2.39 (< 0.001)
10-nonadecenoate (19:1n9)	1.88 (< 0.001)	2.29 (< 0.001)	1.83 (< 0.001)	1.96 (< 0.001)
arachidate (20:0)	1.43 (0.049)	1.97 (< 0.001)	1.26 (0.235)	1.49 (0.026)
eicosenoate (20:1n9 or 11)	1.93 (< 0.001)	2.8 (< 0.001)	1.91 (< 0.001)	2.19 (< 0.001)
dihomo-linoleate (20:2n6)	1.98 (< 0.001)	2.27 (< 0.001)	2.09 (< 0.001)	2 (< 0.001)
arachidonate (20:4n6)	1.69 (< 0.001)	2 (< 0.001)	1.63 (< 0.001)	1.85 (< 0.001)
behenate (22:0)	1.75 (0.026)	2.53 (< 0.001)	1.22 (0.610)	1.73 (0.009)
docosadienoate (22:2n6)	2.26 (< 0.001)	2.66 (< 0.001)	1.93 (< 0.001)	2.23 (< 0.001)
adrenate (22:4n6)	2.55 (0.007)	2.55 (0.009)	1.68 (0.085)	3.2 (0.002)
lignocerate (24:0)	1.02 (0.991)	1.16 (0.398)	1.06 (0.741)	1.15 (0.642)
azelate (nonanedioate)	2.36 (< 0.001)	1.99 (< 0.001)	1.87 (0.179)	1.94 (0.002)
hexanoylcarnitine	0.54 (< 0.001)	0.82 (0.062)	0.69 (0.001)	0.83 (0.089)
octanoylcarnitine	0.62 (< 0.001)	0.71 (< 0.001)	0.74 (0.002)	0.68 (< 0.001)
palmitoylcarnitine	0.6 (0.034)	0.15 (< 0.001)	0.29 (< 0.001)	0.15 (< 0.001)
stearoylcarnitine	0.7 (0.083)	0.25 (< 0.001)	0.4 (< 0.001)	0.24 (< 0.001)
oleoylcarnitine	0.37 (< 0.001)	0.09 (< 0.001)	0.18 (< 0.001)	0.1 (< 0.001)
carnitine	0.07 (< 0.001)	0.06 (< 0.001)	0.09 (< 0.001)	0.05 (< 0.001)
nicotinamide	1.33 (0.036)	0.91 (0.437)	1.09 (0.555)	0.82 (0.165)
nicotinamide adenine dinucleotide (NAD^+)	0.52 (< 0.001)	0.29 (< 0.001)	0.52 (< 0.001)	0.29 (< 0.001)
nicotinamide adenine dinucleotide reduced (NADH)	0.65 (0.003)	0.66 (0.006)	0.71 (0.016)	0.4 (< 0.001)
nicotinate adenine dinucleotide ($NAAD^+$)	0.41 (< 0.001)	0.34 (< 0.001)	0.57 (< 0.001)	0.38 (< 0.001)
pantothenate	0.43 (< 0.001)	0.24 (< 0.001)	0.32 (< 0.001)	0.22 (< 0.001)
phosphopantetheine	0.33 (< 0.001)	0.81 (0.383)	0.4 (< 0.001)	0.83 (0.516)
coenzyme A	0.4 (< 0.001)	0.5 (< 0.001)	0.39 (< 0.001)	0.44 (< 0.001)
3’-dephosphocoenzyme A	0.44 (< 0.001)	0.55 (0.001)	0.43 (< 0.001)	0.59 (0.004)

[a]Results indicate the mean fold difference; P values from ANOVA comparisons are in parentheses.